Power Delay Profile Based Ranging via Approximate EM-ReVAMP

Fangqing Xiao, Zilu Zhao, Dirk Slock

Power Delay Profile Based Ranging via Approximate EM-ReVAMP

Fangqing Xiao, Zilu Zhao, Dirk Slock
Communication Systems Department, EURECOM, France
fangqing.xiao@eurecom.fr, zilu.zhao@eurecom.fr, dirk.slock@eurecom.fr

***Abstract*—Accurate distance estimation is of utmost importance in enabling seamless positioning and location-based services for 5G and Beyond 5G (B5G) networks. This paper focuses on addressing the ranging problem caused by multipath propagation, utilizing the widely adopted Nakagami-m amplitude fading model. We propose a novel method for estimating range based on Multipath Components (MPCs), establishing a relationship between the distribution parameters and propagation distance. To address the estimation problem within the MPCs-based ranging method, we employ the Expectation Maximization (EM)-Revisited Approximate Message Passing (ReVAMP) algorithm. This algorithm is specifically designed to handle challenges in parameter estimation for generalized linear models (GLMs) with hidden random variables and intractable posterior distributions during EM iterations. Simulation results have been conducted to prove the accuracy and robustness of our ranging method, which consistently confirm its effectiveness.**

***Index Terms*—Ranging Estimation, Multipath Components, Expectation Maximization, Revisited Approximate Message Passing Algorithm**

I. Introduction

With the rapid advancement of communication techniques, localization estimation has emerged as a critical aspect in fifth-generation (5G) and beyond 5G (B5G) networks [1]. Many distance-based positioning protocols rely on the received signal strength indicator (RSSI) to estimate position via analyzing the power level received by the receiver [2]–[4]. However, it was asserted that RSSI is not an ideal metric due to its vulnerability to multipath effects [5], [6]. In complex environments, the receiver may encounter multiple signals arriving through different paths, including line-of-sight (LoS) and non-line-of-sight (NLoS) paths, which significantly intensifies the multipath effect shown as Fig. 1. Consequently, establishing a straightforward relationship between received power and propagation distance becomes impractical [7].

Since RSSI is not applicable in scenarios involving LoS path and a large number of NLoS paths, several studies have aimed to establish empirical models that differentiate between their power attenuation in relation to propagation distance [8]–[10]. One widely accepted propagation model for indoor multipath propagation is the Saleh-Valenzuela model [9], which takes into account factors such as reflection, diffraction, and scattering caused by indoor structures. However, this model may not accurately represent channel behavior in outdoor or wide-area environments, as it does not explicitly consider wide-area path loss, shadowing, and

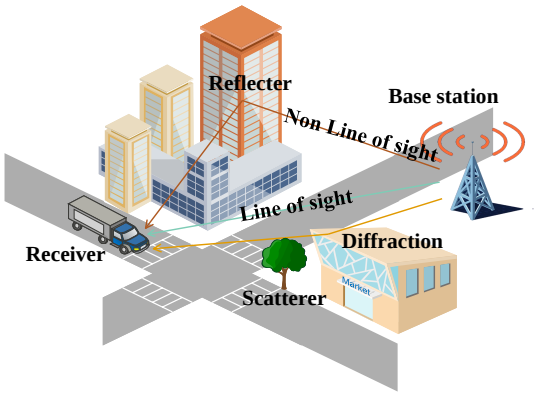

Fig. 1. Example of LoS and NLoS links.

other outdoor-specific phenomena [11]. To accurately model outdoor or wide-area channel behavior, different empirical models or models based on extensive outdoor measurements, such as the Okumura-Hata model [12] or the 3GPP model [13], are commonly used. However, establishing a generic attenuation model for each MPC with respect to (w.r.t.) the propagation distance is not adequately accounted for.

To address these challenges, our initial focus was on selecting a suitable model that accurately captures the decay of MPCs. After a comprehensive evaluation, we concluded that the Nakagami-m distribution is well-suited for representing the amplitude fading of each MPC, taking into account the uniform distribution of the phase varying from 0 to 2π [14]. In comparison to alternative models like Rayleigh, Rician, or log-normal distributions, the Nakagami-m distribution demonstrated superior versatility and accuracy in fitting a wide range of experimental data [15]. This superiority stems from its capability to accommodate the superposition of primary and clutter signals resulting from diffuse reflections within a single path, making it a better fit than the Rayleigh distribution [14]. It is worth noting that both the Rician and Nakagami distributions exhibit similar characteristics at the mean attachment point.

Furthermore, we considered how to establish the relationship between the parameters of the Nakagami-m distribution and the propagation distance to enable distance estimation. The parameter m is closely associated with the environment, while Ω represents the average attenuation power intensity [16], which is directly linked to the propagation distance.

Consequently, when the received data contains sufficient information about the attenuation of different paths, we can directly estimate the distance based on these measurements. While previous studies [17]–[19] have explored the use of MPCs for localization estimation, to the best of our knowledge, no prior research has specifically focused on directly estimating the propagation distance of the LoS path by assuming that both the LoS and NLoS paths conform to specific fading distributions.

For range estimation utilizing MPCs with Nakagami-m amplitude fading, we formulate the problem of range estimation and propose the EM-ReVAMP algorithm as an effective solution. The EM algorithm is employed to handle a GLM that incorporates hidden variables. In cases where the analytic formula for the posterior probability density function (PDF) is unavailable within the EM algorithm, we introduce the ReVAMP inference algorithm to approximate the posterior distribution. The simulations demonstrate that the MPCs-based ranging exhibits high accuracy and robustness. Our ranging method serves as a foundation for precise distance estimation and further positioning in wireless communication networks, thereby enhancing performance and improving user experiences.

The organization of the remaining sections is as follows: Section II presents the system model, encompassing the orthogonal frequency-division multiplexing (OFDM) model, Nakagami-m amplitude fading of MPCs, and MPCs-based ranging estimation. Sections III and IV delve into explanations of the EM algorithm and the ReVAMP algorithm, respectively. In Section V, we describe the procedure for estimating distance using the EM-ReVAMP algorithm. Subsequently, Section VI showcases the simulation results. Finally, Section VII concludes with our findings and conclusions.

Notation: The following notation will be used throughout this paper. Column vectors are denoted by lowercase bold $\boldsymbol{x}$. Matrices are denoted by uppercase bold $\boldsymbol{X}$. Scalars are represented without bold, such as x. The i^{th} entry of a vector $\boldsymbol{x}$ is designated as $x[i]$ or x_i. The element at row i and column j of matrix $\boldsymbol{X}$ is denoted as X_{ij}.The operation $diag(\boldsymbol{X})$ is used to extract the column vector consisting of the main diagonal elements of the matrix $\boldsymbol{X}$.

II. System model

In this section, we will offer a succinct introduction to the system model.

A. OFDM model

The widely preferred modulation technique in communication networks is OFDM, which finds extensive application in 5G-NR [20]. In the OFDM model, the received baseband signal can be mathematically expressed as the convolution of the transmitted OFDM signal, denoted as $s(t)$, and the channel impulse response, denoted as $g(t)$. Additionally, complex additive white Gaussian noise, represented as $v(t)$, is added to the received signal. This relationship can be represented as:

$$r(t) = s(t) * g(t) + v(t), \tag{1}$$

where * denotes the convolution operation. After the received signal, $r(t)$, is sampled at a rate of T_s, time and frequency synchronizations are performed prior to the N-point fast Fourier transform (FFT) operation. The output of the FFT, denoted as $\mathbf{y}$, can be written as:

$$\boldsymbol{y} = \boldsymbol{X}\boldsymbol{h} + \boldsymbol{v} \in \mathcal{C}^{N\times 1}, \tag{2}$$

where $\boldsymbol{X}$ is an $N \times N$ diagonal matrix containing the transmitted pilot symbols on its diagonal, $\boldsymbol{h}$ represents the channel frequency response (CFR) as a vector, and $\boldsymbol{v}$ is a vector of independently and identically distributed (i.i.d.) complex zero-mean Gaussian noise samples with equal variance σ_v^2.

In the case of a block fading channel that remains constant over the duration of a packet, the channel impulse response (CIR) can be described as follows: [21]

$$g(t) = \sum_{l=0}^{L-1} a_l \delta(t - \kappa_l T_s), \tag{3}$$

where a_l and $\kappa_l T_s (\kappa_0 < \kappa_1 < ... < \kappa_{L-1})$ represent the gain and delay of the l^{th} path, respectively, and $\delta(t)$ denotes the Kronecker delta function. Let

$$\boldsymbol{h} = [h_0,\ h_1,\ ...\ ,\ h_{N-1}]^T, \tag{4}$$

be the discrete CFR, where $()^T$ represents the transpose of $()$. Under the assumption that the sampling starts at $t = 0$, the n th element of $\boldsymbol{h}$ can be written as: [22]

$$h_n = \sum_{l=0}^{L-1} a_l e^{-j\kappa_l\omega}\big|_{\omega=\frac{2\pi[n]_N}{N}}, \tag{5}$$

where

$$[n]_N = \begin{cases} n, & n \le N/2 - 1, \\ n - N, & n \ge N/2 + 1. \end{cases} \tag{6}$$

Therefore, we can present (5) as

$$\boldsymbol{h} = \boldsymbol{T}\boldsymbol{a} \in \mathcal{C}^{N\times 1} \tag{7}$$

where $\boldsymbol{a} \in \mathcal{C}^{L\times 1}$ is a vector filled with fading gains and $\boldsymbol{T} \in \mathcal{C}^{N\times L}$ is a transformation matrix that $T_{kl} = e^{-j\kappa_l\omega}\big|_{\omega=\frac{2\pi[k]_N}{N}}$.

B. Nakagami-m amplitude fading of MPCs

As discussed in the previous subsection, the received signal in OFDM can be represented as follows:

$$\boldsymbol{y} = \boldsymbol{X}\boldsymbol{T}\boldsymbol{a} + \boldsymbol{v} = \boldsymbol{H}\boldsymbol{a} + \boldsymbol{v}; \quad \boldsymbol{v} \sim \mathcal{CN}(0, \sigma_v^2\mathbf{I}), \tag{8}$$

where $\boldsymbol{a} \in \mathcal{C}^{N\times 1}$ denotes the complex attenuation coefficients (amplitude $\boldsymbol{m}$ and phase $\boldsymbol{\phi}$). For each individual element $a_i = m_i e^{j\phi_i}$ of $\boldsymbol{a}$, we assume its magnitude m_i with a Nakagami-m distribution and phase ϕ_i with a uniform distribution. Therefore, the PDF of magnitude and phase can be expressed as follows:

$$p(m_i|\Omega_i) = \frac{2m^m m_i^{2m-1}}{\Gamma(m)\,\Omega_i^m} \exp\left[-\frac{m\,m_i^2}{\Omega_i}\right], m_i > 0; \tag{9a}$$

$$p(\phi_i) = \frac{1}{2\pi}, \quad \phi_i \in [0, 2\pi), \tag{9b}$$

where $\Gamma(\cdot)$ denotes the gamma function m is the shape parameter of the Nakagami-m distribution and Ω_i is the average power intensity of path i. The shape parameter m controls the fading characteristics of the distribution. For lower values of m, the distribution resembles a Rayleigh distribution with a more rapid decay. As m increases, the distribution becomes more concentrated around its mean, resembling a more concentrated fading behavior. In practice, m is often estimated from channel measurements to accurately model the fading characteristics of the specific wireless channel. Referring to [23], the parameter Ω_i can be defined as:

$$\Omega_i(d_0) = P_t G_t G_r \left[\frac{\lambda}{4\pi(d_0 + c\tau_i)}\right]^n = G_0(d_0 + c\tau_i)^{-n}, \tag{10}$$

in the given equation, several variables are defined as follows: P_t represents the transmitting power, G_t denotes the transmitting antenna amplification, λ is the wavelength of the electromagnetic wave, c is the velocity of light, n represents the propagation fading factor influenced by the environment, d_0 indicates the LoS distance, and τ_i indicates the propagation delay between the i-th path and the LoS path.

In (10), the term $P_t G_t G_r \left(\frac{\lambda}{4\pi}\right)^n$ can be considered as a constant, denoted as G_0, which combines the effects of transmit power, antenna gains, wavelength, and path loss exponent. The propagation fading factor n plays a crucial role in determining the rate of signal attenuation with distance and can vary depending on the characteristics of the wireless channel and the environment in which the signals propagate. As the propagation distance $d_0 + c\tau_i$ increases, Ω_i decreases following an inverse power-law relationship $(d_0 + c\tau_i)^{-n}$. This allows us to estimate the specific range d_0 based on Ω_i when τ_i is known in a given environment.

Using the Jacobi determinant, we can obtain the PDF of the complex fading coefficient a_i as follows:

$$p(a_i|\Omega_i(d_0)) = \frac{m^m |a_i|^{2m-2}}{\pi\,\Gamma(m)\,\Omega_i^m} \exp\left[-\frac{m\,|a_i|^2}{\Omega_i}\right], m \geq 0.5. \tag{11}$$

For simplicity, we denote $p(a_i|d_0)$ by $p(a_i|\Omega_i(d_0))$. Thus, the PDF of the collection $\boldsymbol{a}$ can be given as:

$$p(\boldsymbol{a}|d_0) = \prod_{i=0}^{L-1} p(a_i|d_0). \tag{12}$$

In this estimation process, we assume the presence of a LoS path with an unknown distance d_0, as well as measurable time delay between NLoS paths and the LoS path. While there may be some measurement bias, it is relatively negligible compared to the bias associated with estimating the distance d_0. Hence, we can disregard these biases in the subsequent estimation process.

C. MPCs-based Ranging Estimation

Our objective is to estimate d_0 directly from $\boldsymbol{y}$. To achieve this, we will employ the maximum likelihood estimation (MLE) method, which transforms the problem into the following equation:

$$\hat{d_0} = \arg\max_{d_0} \ell(d_0; \boldsymbol{y}) = \arg\max_{d_0} \ln \mathcal{L}(d_0; \boldsymbol{y}), \tag{13}$$

where $\mathcal{L}(\cdot)$ and $\ell(\cdot)$ represent the likelihood function and log-likelihood function, respectively.

Regarding the optimization problem (13), the likelihood function can be expressed as:

$$\mathcal{L}(d_0; \boldsymbol{y}) = p(\boldsymbol{y}|d_0) = \int p(\boldsymbol{a}, \boldsymbol{y}|d_0) d\boldsymbol{a} = \int p(\boldsymbol{y}|\boldsymbol{a}) p(\boldsymbol{a}|d_0) d\boldsymbol{a}. \tag{14}$$

The PDF $p(\boldsymbol{y}|d_0)$ is crucial for estimating the LoS range d_0 based on the received signal $\boldsymbol{y}$ in 13. However, solving the integral problem directly to acquire $p(\boldsymbol{y}|d_0)$ proves to be intractable, as finding an analytical form poses significant challenges. In the next sections, a subtle algorithm is leveraged to solve this puzzle.

III. Review of Expectation Maximization (EM)

As we discussed before, in the linear mixing data model described by equation (8), we have a known measurement matrix $\boldsymbol{H} \in \mathcal{C}^{M \times L}$ and an independent and non-identically distributed (n.i.i.d.) prior $p(\boldsymbol{a}|d_0) = \prod_{i=0}^{L-1} p(a_i|d_0)$ for the vector $\boldsymbol{a}$. Additionally, we consider a zero-mean Gaussian measurement noise $p(\boldsymbol{v}) = \mathcal{CN}(\boldsymbol{v}; \boldsymbol{0}, \boldsymbol{C}_{vv})$ with covariance matrix $\boldsymbol{C}_{vv} \in \mathcal{R}^{M \times M}$.

To address the optimization problem (13), the Expectation-Maximization (EM) algorithm [24] proves to be a suitable solution. This algorithm is effective for estimation problems involving latent variables, such as $\boldsymbol{a}$, which are unobserved.

According to (14), the Log-Likelihood of d_0 can be presented as

$$\ell(d_0; \boldsymbol{y}) = \ln p(\boldsymbol{y}|d_0) = \ln \int p(\boldsymbol{y}|\boldsymbol{a}) p(\boldsymbol{a}|d_0) d\boldsymbol{a} \tag{15}$$

As discussed in (13), the parameters d_0 estimation becomes maximizing the log-likelihood

$$\hat{d_0} = \arg\max_{d_0} \ell(d_0). \tag{16}$$

Direct optimization of the log-likelihood may be very difficult. One approach is to do minorization maximization (MM) [25] in which we construct a more easily optimized lower bound of the log-likelihood function and iteratively approximate the optimal parameters by continuously optimizing this lower bound. When considering the Nakagami-m prior distribution of $\boldsymbol{a}$ as described in equation (12), the EM iteration can be expressed as follows:

$$\begin{aligned} d_0^{(t+1)} &= \arg\max_{d_0} \mathcal{E}_{p(\boldsymbol{a}|\boldsymbol{y}, d_0^{(t)})} \left[\sum_{i=0}^{L-1} (-\ln \Omega_i(d_0) - \frac{|a_i|^2}{\Omega_i(d_0)})\right] \\ &= \arg\min_{d_0} \sum_{i=0}^{L-1} \left[\ln \Omega_i(d_0) + \frac{\mathcal{E}_{p(\boldsymbol{a}|\boldsymbol{y}, d_0^{(t)})}\left[|a_i|^2\right]}{\Omega_i(d_0)})\right], \end{aligned} \tag{17}$$

where $\Omega_i(d_0)$ was defined in (10). However, in this scenario, the EM algorithm remains intractable because obtaining the posterior distribution $p(\boldsymbol{a}|\boldsymbol{y}, d_0^{(t)})$ is challenging due to

the integration. Therefore, it becomes crucial to develop an algorithm that approximates this posterior distribution with another tractable distribution. To achieve this goal, we propose an algorithm called Revisited Approximate Message Passing (ReVAMP).

IV. Revisited Approximate Message Passing (ReVAMP)

The purpose of the ReVAMP algorithm is to find a complex Gaussian distribution $\mathcal{N}(\boldsymbol{a}; \boldsymbol{m}, \boldsymbol{C}_m)$ approximating the posterior $p(\boldsymbol{a}|\boldsymbol{y}, d_0^{(t)})$ where $d_0^{(t)}$ is known, as

$$p(\boldsymbol{a}|\boldsymbol{y}, d_0^{(t)}) = \frac{p(\boldsymbol{y}, \boldsymbol{a}|d_0^{(t)})}{\int p(\boldsymbol{y}, \boldsymbol{a}|d_0^{(t)}) d\boldsymbol{y}} \approx q(\boldsymbol{a}) = \mathcal{CN}(\boldsymbol{a}; \boldsymbol{m}, \boldsymbol{C}_m). \tag{18}$$

To obtain $\boldsymbol{m}$ and $\boldsymbol{C}_m$, in the linear mixing data model (8), we factorize the approximate distribution as:

$$q(\boldsymbol{a}) = \prod_{i=0}^{L-1} q(a_i) \propto p(\boldsymbol{y}|\boldsymbol{a}) \prod_{i=0}^{L-1} f_i(a_i), \tag{19}$$

where $f_{a_i}(a_i)$ is supposed to be complex gaussian. The Expectation Propagation (EP)-liked form of ReVAMP is given as:

1) Initialize the factors: $f_i(a_i)$
2) Compute the posterior for $\boldsymbol{a}$ from the product of $f_i(a_i)$:

$$q(\boldsymbol{a}) = \frac{p(\boldsymbol{y}|\boldsymbol{a}) \prod_{i=0}^{L-1} f_i(a_i)}{\int p(\boldsymbol{y}|\boldsymbol{a}) \prod_{i=0}^{L-1} f_i(a_i) d\boldsymbol{a}}. \tag{20}$$

3) Until all $f_i(a_i)$ converge:
   a) Choose a $f_i(a_i)$ to refine
   b) Remove $f_i(a_i)$ from the posterior and integral out $\boldsymbol{a}$ except a_i to get an extrinsic:

$$b(a_i) = \int \frac{q(\boldsymbol{a})}{f_i(a_i)} d\boldsymbol{a}_{\setminus i}. \tag{21}$$

   c) Combine with real prior $p(a_i|d_0^{(t)})$ and minimize Kullback–Leibler (KL) divergence to get an approximate marginal posterior $\hat{q}(a_i)$:

$$\hat{q}(a_i) = \arg\min_{q(a_i)} D_{KL}\left[b(a_i) p(a_i|d_0^{(t)}) || q(a_i)\right]. \tag{22}$$

   d) Update $\hat{f}_i(a_i) \propto \hat{q}(a_i)/b(a_i)$

4) Generate an approximated posterior $\hat{q}(\boldsymbol{a})$:

$$\hat{q}(\boldsymbol{a}) = \frac{p(\boldsymbol{y}|\boldsymbol{x}) \prod_{i=0}^{L-1} \hat{f}_i(a_i)}{\int p(\boldsymbol{y}|\boldsymbol{x}) \prod_{i=0}^{L-1} \hat{f}_i(a_i) d\boldsymbol{a}}. \tag{23}$$

This algorithm always has a fixed point with gaussian approximation factors and if initialized too far away from a fixed point, it may diverge [26]. ReVAMP is an EP-liked algorithm that extends the VAMP algorithm, and for more comprehensive insights into the inner workings, refer to their respective research papers [26]–[28].

Algorithm 1 EM-ReVAMP

Ensure: $\hat{d}_0$
Require: $\boldsymbol{y}$, $\boldsymbol{H}$, $p_{\boldsymbol{v}}(\boldsymbol{v})$, G_0, $\boldsymbol{\tau}$
Initialize: $\hat{d}_0$
repeat [For $t = 0 \dots L-1$]
Initialize: $\boldsymbol{C}_p$, $\boldsymbol{p}$
  repeat
    repeat [For $i = 1 \dots N$]
      [Update the posterior approximation]
      $\boldsymbol{C}_{\boldsymbol{a}} = \left(\boldsymbol{H}^H \boldsymbol{C}_{vv}^{-1} \boldsymbol{H} + \boldsymbol{C}_p^{-1}\right)^{-1}$
      $\hat{\boldsymbol{a}} = \boldsymbol{C}_{\boldsymbol{a}} \left(\boldsymbol{H}^H \boldsymbol{C}_{vv}^{-1} \boldsymbol{y} + \boldsymbol{C}_p^{-1} \boldsymbol{p}\right)$
      [Update the extrinsic]
      $r_i = \frac{C_{p_{ii}} a_i - C_{a_{ii}} p_i}{C_{p_{ii}} - C_{a_{ii}}}$
      $\tau_{r_i} = \frac{C_{p_{ii}} C_{a_{ii}}}{C_{p_{ii}} - C_{a_{ii}}}$
      [Gaussian marginal posterior approximation]
      $\hat{a}_i = \frac{\int a_i p(a_i|\hat{d}_0) \mathcal{CN}(a_i; r_i, \tau_{r_i}) da_i}{\int p(a_i|\hat{d}_0) \mathcal{CN}(a_i; r_i, \tau_{r_i}) da_i}$
      $C_{a_{ii}} = \frac{\int |a_i - \hat{a}_i|^2 p(a_i|\hat{d}_0) \mathcal{CN}(a_i; r_i, \tau_{r_i}) da_i}{\int p(a_i|\hat{d}_0) \mathcal{CN}(a_i; r_i, \tau_{r_i}) da_i}$
      [Resulting Gaussian prior approximation]
      $p_i = \frac{\tau_{r_i} \hat{a}_i - C_{a_{ii}} r_i}{\tau_{r_i} - C_{a_{ii}}}$
      $C_{p_{ii}} = \frac{\tau_{r_i} C_{a_{ii}}}{\tau_{r_i} - C_{a_{ii}}}$
    until All i-s have been updated
  until Convergence
  $\hat{d}_0 = \arg\min_{d_0} \sum_{i=0}^{L-1} \left[\ln \Omega_i(d_0) + \frac{C_{a_{ii}} + |\hat{a}_i|^2}{\Omega_i(d_0)})\right]$
until Convergence

V. Ranging estimation with Nakagami-m prior distribution

We propose the EM-ReVAMP algorithm, outlined in Algorithm 1, for estimating d_0. This algorithm utilizes ReVAMP sequentially at each step of the EM algorithm to obtain approximate second-order moments. Specifically, within the ReVAMP part, the marginal posterior approximation involves the calculation of $\hat{a}_i$ and τ_{a_i}, which can be computed as follows:

$$\hat{a}_i = \frac{m d_0^{(t)} r_i}{m\tau_i + d_0^{(t)}} \frac{{}_1F_1(m+1; 2; \frac{d_0^{(t)} |r_i|^2}{m\tau_i^2 + \tau_i d_0^{(t)}})}{{}_1F_1(m; 1; \frac{d_0^{(t)} |r_i|^2}{m\tau_i^2 + \tau_i d_0^{(t)}})}, \tag{24a}$$

$$\tau_{a_i} = \frac{m d_0^{(t)} \tau_i}{m\tau_i + d_0^{(t)}} \frac{{}_1F_1(m+1; 1; \frac{d_0^{(t)} |r_i|^2}{m\tau_i^2 + \tau_i d_0^{(t)}})}{{}_1F_1(m; 1; \frac{d_0^{(t)} |r_i|^2}{m\tau_i^2 + \tau_i d_0^{(t)}})} - \hat{a}_i \hat{a}_i^*, \tag{24b}$$

where ${}_1F_1(a; b; z)$ represents the confluent hypergeometric function [29], defined by the hypergeometric series:

$${}_1F_1(a; b; z) = \sum_{k=0}^{\infty} \frac{(a)_k}{(b)_k} \frac{z^k}{k!}. \tag{25}$$

VI. Simulation Results

This section presents the simulation verification using MATLAB to assess the impact of different parameters. Table I lists the main parameters involved. In general, the main environmental influences on MPCs-based ranging are the number of distinguishable MPCs, the magnitude of the Signal-to-Noise Ratio (SNR), the propagation attenuation

TABLE I
PARAMETERS SETTING

Parameter	Value
G_0	1.
SNR (dB)	Range from 10 to 30, default 20.
N	10.
L	Ranging from 2 to 4
n	Ranging from 2 to 4, default 3.
m	Ranging from 0.5 to 2, default 1.
d_0 (meter)	10.
Distance of NLOS path (m)	Random between $1.1d_0$ to $2.0d_0$.
Test repetitions	20.

factor n, and the shape parameter of Nakagami-m distribution m. In the following subsection, we analyze the effects of these factors on ranging accuracy through simulations. We conducted 20 times for each test and calculated the average of the absolute values of the bias.

A. Impact of SNR and Number of NLoS Paths

In this set of experiments, we examine the influence of SNR and the number of NLoS paths on the estimation bias. Fig. 2 illustrates the simulation results. The average estimated errors were 2.8m, 0.7m and 0.1m when there were one NLoS and two NLoS and three NLoS, respectively. We observe that varying SNR from 10dB to 30dB does not significantly affect our performance. However, the estimation accuracy gradually improves with an increasing number of NLoS paths. This finding demonstrates that our algorithm maintains good estimation performance even at low SNR levels.

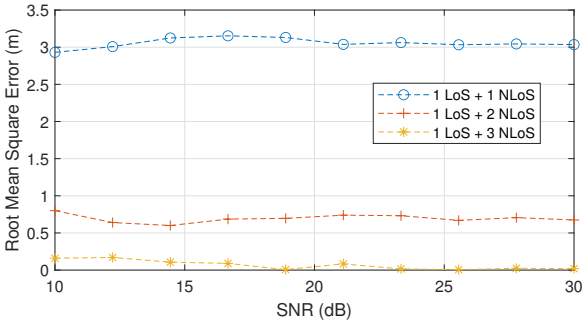

Fig. 2. The impact of SNR and the number of NLoS paths on d_0 estimation

B. Impact of the propagation fading factor n and Number of NLoS Paths

This set of experiments investigates the effects of the environmental propagation fading factor n and the number of NLoS paths on the estimation bias. The simulation results, depicted in Fig. 3, indicate that the variation of n within the range of 2 to 4 has a negligible impact on our performance. The average estimated errors were 2.9m, 0.7m and 0.2m when there were one NLoS and two NLoS and three NLoS, respectively. These results suggest that our algorithm exhibits robust estimation performance even in complex environments, with estimation accuracy gradually improving as the number of NLoS paths increases.

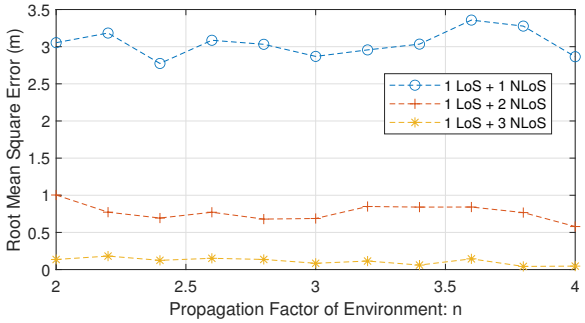

Fig. 3. The impact of the environment propagation fading factor n and the number of NLoS paths on d_0 estimation

C. Impact of the shape parameter m and Number of NLoS Paths

We examine the influence of the shape parameter of the Nakagami-m distribution, denoted as m, and the number of NLoS paths on the estimation bias. Fig. 4 presents the simulation results, indicating that varying m from 0.5 to 2 does not significantly affect our performance. The average estimated errors were 3.0m, 0.7m and 0.2m when there were one NLoS and two NLoS and three NLoS, respectively. These findings highlight the favorable theoretical estimation performance of our algorithm even in complex environments, with the accuracy of estimation gradually improving as the number of NLoS paths increases.

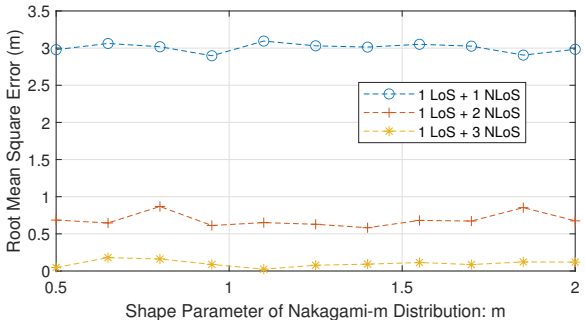

Fig. 4. The impact of the Nakagami-m distribution's shape parameter m and the number of NLoS paths on d_0 estimation

D. Simulation Conclusions

Based on the experimental simulations conducted with varying SNR, values of n and m, and the number of NLoS paths, our method has demonstrated strong performance in diverse and complex environments. Notably, the number of NLoS paths has emerged as a crucial parameter, significantly influencing the accuracy of our estimation. As the number of NLoS paths increases, the accuracy of our algorithm improves. Because the accuracy of the estimation is directly linked to the availability of eligible samples. Consequently, a higher number of eligible samples leads to improved estimation accuracy. The number of eligible samples used in the estimation is the primary determinant of the accuracy of our range estimation algorithm when the SNR is not

particularly small. Hence, in complex environments characterized by a substantial multipath component, the EM-ReVAMP algorithm proves to be an effective solution for estimating the LoS distance.

VII. Conclusions

We propose a novel method for precise range estimation within multipath propagation, aimed at overcoming the associated challenges. Our approach utilizes the widely adopted Nakagami-m amplitude fading model and establishes a relationship between distribution parameters and propagation distance. To address the challenge of parameter estimation for GLMs that involve hidden random variables and intractable posterior distributions in the context of our range estimation method, we introduce the EM-ReVAMP algorithm. The simulation results convincingly demonstrate the accuracy and robustness of our approach, providing substantial evidence to support the effectiveness of the EM-ReVAMP algorithm. To further validate the practicality and effectiveness of our method, our next objective is to gather measurement data from diverse environments and conduct thorough experimental analysis. This crucial step will enable us to evaluate the performance of our method in real-world scenarios. Additionally, exploring additional application scenarios of EM-ReVAMP and investigating its theoretical performance are vital aspects that require attention.

Acknowledgements EURECOM's research is partially supported by its industrial members: ORANGE, BMW, SAP, iABG, Norton LifeLock, and by the Franco-German projects 5G-OPERA and CellFree6G.

References

[1] F. Mogyorósi *et al.*, "Positioning 5g and 6g networks—a survey," *Sensors*, vol. 22, no. 13, p. 4757, 2022.

[2] G. Zanca, F. Zorzi, A. Zanella, and M. Zorzi, "Experimental comparison of rssi-based localization algorithms for indoor wireless sensor networks," in *Proc. IEEE WWSN*, 2008, pp. 1–5.

[3] H. P. Mistry and N. H. Mistry, "Rssi-based localization scheme wireless sensor networks: A survey," in *Proc. IEEE ACCT*, 2015.

[4] Z. Yang, Z. Zhou, and Y. Liu, "From rssi to csi: Indoor localization via channel response," *ACM Comput. Surv. (CSUR)*, vol. 46, no. 2, pp. 1–32, 2013.

[5] T. Nowak, M. Hartmann, H.-M. Tröger, L. Patino-Studencki, and J. Thielecke, "Probabilistic multipath mitigation rssi-based direction-of-arrival estimation," in *Proc. IEEE ICC Workshop*, 2017, pp. 1024–1029.

[6] T. Aono, K. Higuchi, T. Ohira, B. Komiyama, and H. Sasaoka, "Wireless secret key generation exploiting reactance-doma scalar response of multipath fading channels," *IEEE Trans. Antennas Propag.*, vol. 53, no. 11, pp. 3776–3784, 2005.

[7] F. Carpi *et al.*, "Rssi-based methods for los/nlos channel identification indoor scenarios," in *Proc. IEEE ISWCS*, 2019.

[8] T. S. Rappaport *et al.*, "Wideband millimeter-wave propagation measurements and channel models for future wireless communication system design," *IEEE Trans. Commun.*, vol. 63, no. 9, pp. 3029–3056, 2015.

[9] A. A. Saleh and R. Valenzuela, "A statistical model for indoor multipath propagation," *IEEE J. Sel. Areas Commun.*, vol. 5, no. 2, pp. 128–137, 1987.

[10] F.-J. O. Juliet and W. Stuart, "Empirical investigation of indoor/nlos propagation at millimeter wave bands for gigabits throughput realization: 24 and 60ghz links."

[11] A. Meijerink and A. F. Molisch, "On the physical interpretation of the saleh–valenzuela model and the definition of its power delay profiles," *IEEE Trans. Antennas Propag.*, vol. 62, no. 9, pp. 4780–4793, 2014.

[12] A. Medeisis and A. Kajackas, "On the use of the universal okumura-hata propagation prediction model rural areas," in *Proc. IEEE VTC*, vol. 3, 2000.

[13] D. S. Baum *et al.*, "An interim channel model for beyond-3g systems: Extending the 3gpp spatial channel model (scm)," in *Proc. IEEE VTC*, vol. 5, 2005.

[14] H. Stefanovic, A. Savic *et al.*, "Some general characteristics of nakagami-m distribution," in *Proc. ISCIM*, 2011, pp. 721–731.

[15] S. M. Abuelenin, "On the similarity between nakagami-m fading distribution and the gaussian ensembles of random matrix theory," *arXiv:1803.08688*, 2018.

[16] N. C. Beaulieu and C. Cheng, "Efficient nakagami-m fading channel simulation," *IEEE Trans. on Vehicular Technology*, vol. 54, no. 2, pp. 413–424, 2005.

[17] K. Wu *et al.*, "Csi-based indoor localization," *IEEE Trans. Parallel Distrib. Syst.*, vol. 24, no. 7, pp. 1300–1309, 2012.

[18] X. Wang, L. Gao, S. Mao, and S. Pandey, "Csi-based fingerprinting for indoor localization: A deep learning approach," *IEEE Trans. Veh. Technol.*, vol. 66, no. 1, pp. 763–776, 2016.

[19] W. Liu *et al.*, "Survey on csi-based indoor positioning systems and recent advances," in *Proc. IPIN*. IEEE, 2019.

[20] A. M. Graff *et al.*, "Analysis of ofdm signals for ranging and communications," in *Proc. Conf. ION GNSS+*, 2021, pp. 2910–2924.

[21] A. Goldsmith, *Wireless communications*. Cambridge university press, 2005.

[22] J. Liu, "Be cautious when using the fir channel model with the ofdm-based communication systems," *IEEE Trans. Veh. Technol.*, vol. 58, no. 3, pp. 1607–1612, 2008.

[23] V. A. Aalo, C. Mukasa, and G. P. Efthymoglou, "Effect of mobility on the outage and ber performances of digital transmissions over nakagami-m fading channels," *IEEE Trans. Veh. Technol.*, vol. 65, no. 4, pp. 2715–2721, 2015.

[24] S. Borman, "The expectation maximization algorithm - a short tutorial," 41, 2004, submitted for publication.

[25] D. R. Hunter and K. Lange, "A tutorial on mm algorithms," *Am. Stat.*, vol. 58, no. 1, pp. 30–37, 2004.

[26] T. P. Minka, "Expectation propagation for approximate bayesian inference," *arXiv:1301.2294*, 2013.

[27] J. P. Cunningham, P. Hennig, and S. Lacoste-Julien, "Gaussian probabilities and expectation propagation," *arXiv:1111.6832*, 2011.

[28] S. Rangan, P. Schniter, and A. K. Fletcher, "Vector approximate message passing," *IEEE Trans. Inf. Theory*, vol. 65, no. 10, pp. 6664–6684, 2019.

[29] H. Buchholz, *The confluent hypergeometric function: with special emphasis on its applications*. SSBM, 2013, vol. 15.